Asian Journal of Scientific Research

ISSN 1992-1454

science alert
http://www.scialert.net

ANSInet
an open access publisher
http://ansinet.com

OPEN ACCESS Asian Journal of Scientific Research

ISSN 1992-1454
DOI: 10.3923/ajsr.2016.176.187

Research Article
Simulation of 416 kHz Piezoelectric Transducer Excitation using Class E ZVS Inverter

[1]H. Husin, [1]S. Saat, [1]Y. Yusmarnita, [1]Z. Ghani, [1]I. Hindustan and [2]S.K. Nguang

[1]Universiti Teknikal Malaysia Melaka, Hang Tuah Jaya, 76100 Durian Tunggal, Melaka, Malaysia
[2]University of Auckland, Victoria Street West, Auckland 1142, New Zealand

Abstract

In Acoustic Energy Transfer (AET) system, piezoelectric transducers played a role in converting the electrical energy to mechanical stress or vice versa. It is required to drive the piezoelectric transducer in the transmitter unit at the exact operating frequency, so that the high efficiency of power conversion can be achieved. This study presents the simulation model of the excitation circuit to drive the piezoelectric transducer using class E ZVS as DC-AC inverter in the transmitter unit of AET system. As design specifications with the PZT transducer operating frequency of 416 kHz, 80 mW power output is aimed from the inverter circuit. Proteus software used as simulation platform with peripheral interface controller (PIC16F877A) as Pulse Width Modulation (PWM) signal generator for MOSFET IRF5852TR. The transmitter unit is modeled in stages started with optimum operation of class E ZVS, followed by the insertion of piezoelectric transducer equivalent circuit and end up with the matching impedance circuit in order to achieve maximum power conversion as the main concerns of this study. The simulation result from the proposed design generates a 72.22 mW with 90.3% efficiency. This signifies that simulation results agree upon the theoretical calculation.

Key words: Acoustic energy transfer, DC-AC transmitter, PWM, piezoelectric transducer, class E ZVS

Received: May 10, 2016 **Accepted:** August 06, 2016 **Published:** September 15, 2016

Citation: H. Husin, S. Saat, Y. Yusmarnita, Z. Ghani, I. Hindustan and S.K. Nguang, 2016. Simulation of 416 kHz piezoelectric transducer excitation using class E ZVS inverter. Asian J. Sci. Res., 9: 176-187.

Corresponding Author: H. Husin, University Teknikal Malaysia Melaka, Hang Tuah Jaya, 76100 Durian Tunggal, Melaka, Malaysia

Competing Interest: The authors have declared that no competing interest exists.

Data Availability: All relevant data are within the paper and its supporting information files.

INTRODUCTION

Numerous established of Wireless Power Transfer (WPT) technologies gained attracting attention from the researcher currently. Not only due to their capabilities to charge consumer home appliances, but also contributes to other technical aspects such as, supplying the power to sensors/transducers embedded in a human body or charging a moving vehicle on the road. The WPT is also implemented in the industries which required the wear of cable slabs to be minimized as reported in Hu *et al.*[1]. A relatively new alternative method is an Acoustic Energy Transfer (AET), which utilizes sound waves or vibration to propagate energy without depending on the electrical connection between the transmitter and receiver unit. The AET comes into the picture of energy transferring technology due to the urgent requirement of alternative methods of powering low power consumption as proposed by Roes *et al.*[2], Sanni and Vilches[3], Ozeri and Shmilovitz[4] and Denisov and Yeatman[5] such as for Implantable Biomedical Devices (IMDs). Zaid *et al.*[6] claimed that other practical alternatives in the same category of AET for powering those devices include: (i) Inductive Energy Transfer (IET), (ii) Capacitive energy transfer (CPT), (iii) Far-field electromagnetic coupling (EM) and (iv) Optical coupling techniques. The IET has gained a huge attention since the systems managed to deliver energy up to 2 m with high efficiency as reported by Karalis *et al.*[7] and Kurs *et al.*[8], but due to magnetic coupling issue, it is not suitable for metal surrounding environment and cause of large eddy current losses as claimed by Roes *et al.*[2], Theodoridis[9] and Liu *et al.*[10]. The CET takes advantages of these limitations due to its nature that exploits an electric field to penetrate through any metal surroundings. The CET has also a good anti-interference ability of the magnetic field as stated by Liu *et al.*[10], Kline *et al.*[11] and Chen-Yang *et al.*[12]. The implementation of CET is limited due to the restriction of distance that can be crossed with it and have been used for very low power delivery applications proposed by Theodoridis[9], Chen-Yang *et al.*[12], Zaid *et al.*[6] and Kline *et al.*[11].

Far-field electromagnetic coupling (EM) is seldom used because of the difficulty in microwaves generation especially when a solid-state RF generator is applied and for IMDs applications, side effect that harmful to the human body. Optical energy transmission uses same principles as EM and has low efficiency whereby up to 50% energy is lost according to Zaid *et al.*[6] and Roes *et al.*[2]. The above mentioned characteristics make acoustics a primary candidate for WPT in low power applications (in range of μW to mW) due to its power transfer efficiency, compactness and electromagnetic immunity as concluded by Jiang *et al.*[13], Miller[14] and Semsudin *et al.*[15].

In AET systems, the piezoelectric transducer plays a major role in converting an electrical energy to pressure energy or vice-versa. The transducer electrical impedance will affect noise performance, driving response, bandwidth and sensitivity as laid by Svilainis and Dumbrava[16]. Thus, it is required to take into consideration the approach to predict the performance of the piezoelectric transducer as a part of the system.

This study presents the working principle of class E Zero Voltage Switching (ZVS) as soft-switching inverter topology in the transmitter unit of AET system due to its capability to produce high efficiency inverter performance. The high efficiency inverter performance is required for two reasons: (1) To drive the piezoelectric (PZT) transducer at the exact operating frequency without introducing harmonic modes so that maximum DC-AC conversion can be achieved and (2) Prolong the low voltage, low power battery's service life that supplied the transmitter unit. However, this study will dealt only with the first reason due to simulation ability.

This study presents and compares the performance of AET transmitter unit for three conditions: (1) With the optimum condition class E ZVS inverter, (2) With the optimum condition class E ZVS inverter attached to PZT equivalent electrical circuit and iii) with the optimum condition class E ZVS attached to PZT equivalent electrical circuit with matching impedance.

AET system: The basic structure of AET system is shown in Fig. 1 that consists of 2 U, primary/transmitter unit and secondary/receiver unit that's been separated by any material that can propagate sound/pressure waves as a transmission medium. In the transmitter unit, the power converter or inverter will converts a dc supply to an ac supply that being injected to piezoelectric transducer. The transducer will converts that energy to pressure wave which is then transmitted wirelessly. The pressure is collected by another transducer at the receiver side that reconverts the energy back into electrical energy and being amplified based on the load requirements. The transmission medium can be ranged for examples metal, air, human tissue and solid wall as long as it can allow the penetration of pressure wave. An AET system can be applied at the various applications such as ultrasonic cleaning, medical ultrasonography, non-destructive testing, distance measurement (sonar), therapeutic ultrasound and ultrasonic welding. Recently, the urgent demand of the alternative recharging method, especially for Implantable Biomedical Devices (IMDs) shows a trend of applying an AET system.

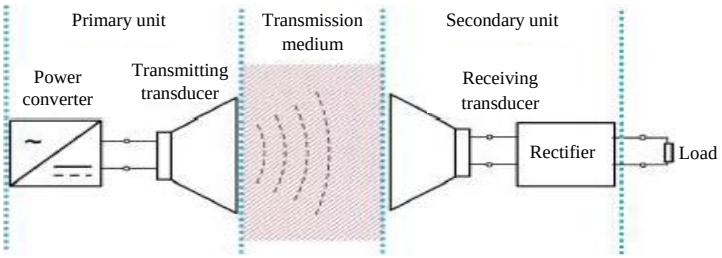

Fig. 1: Basic AET system by Zaid *et al.*[6]

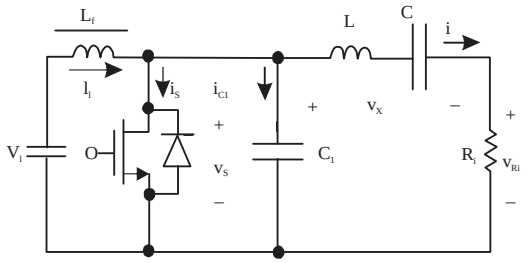

Fig. 2: Class E zero-voltage-switching inverter by Kazimierczuk and Dariusz[18]

Table 1: Load network characteristics

Switch condition	Resonant frequency	Loaded quality factor
Turns on	$f_{01}=\frac{1}{(2\pi\sqrt{LC})}$	$Q_{L1}=\frac{\omega_{01}L}{R_i}=\frac{1}{(\omega_{01}CR_i)}$
Turns off	$f_{02}=\frac{1}{\left[2\pi\sqrt{\frac{LCC_1}{C+C_1}}\right]}$	$Q_{L2}=\frac{\omega_{02}L}{R_i}=\frac{1}{\left[\frac{\omega_{02}LCC_1}{(C+C_1)}\right]}$

CLASS E ZVS INVERTER WORKING PRINCIPLE

Class E ZVS inverters are the most efficient and excellent soft switch inverters circuit, which capable in reducing the voltage stress and switch conduction loss in the resonant circuit as described by Nayak and Reddy[17], Kazimierczuk and Dariusz[18] and Li and Sue[19]. Li and Sue[19] claimed that class E still manageable to operate at the high efficiency even the varying values of resonant components. It can also produce good performance and stability by adjusting the duty cycle and optimizing circuit parameters that supported by Xiaoyuan and Zhe[20]. The current and voltage waveforms of the switch are not overlap during the switching time intervals thus the switching losses are virtually zero, yielding high efficiency. The nature of switching operation that contributing to the high efficiency is controlled by L-C resonant those operate at the instant of zero voltage crossing condition. The circuit diagram is shown in Fig. 2. It consists of power MOSFET that act as a switch, a L-C-R_i series resonant circuit, C_1 as shunt capacitor and L_f as choke inductor. The switch turns on and off at the operating frequency $f = \omega/(2\pi)$ that determined by a driver. The resistor R_i is an AC load.

When the switch is turns on, the resonant circuit consists of L, C and R_i because the capacitance C_1 is short circuited by the switch. However, in the off state, the resonant circuit will consists of C_1, L, C and R_i that connected in series. Thus, the load network can be characterized by two resonant frequencies and two loaded quality factor as tabulated in Table 1.

MATERIALS AND METHODS

The simulations are carried out in three stages:

- Firstly, the transmitter will be equipped with class E ZVS inverter that working at its optimum operation
- Secondly, the first stage is extended with a piezoelectric transducer equivalent circuit to support system level analysis
- Lastly, due to change of AC load value, the matching impedance circuit will be presented at this stage whereby the main objective of the research can be obtained

Stage 1: Optimum operation of class E ZVS

Theoretical calculation of class E ZVS components: In this study, the optimum operation of class E ZVS inverter is studied and simulated. Figure 3 shows the current and voltage waveform for optimum operation. In this case, both the switch voltage v_s and its derivatives d_{vs}/d_t are zero when the switch is turns on. The optimum operation occurred when the maximum drain efficiency is achieved. Due to the derivatives of v_s is zero at the time the

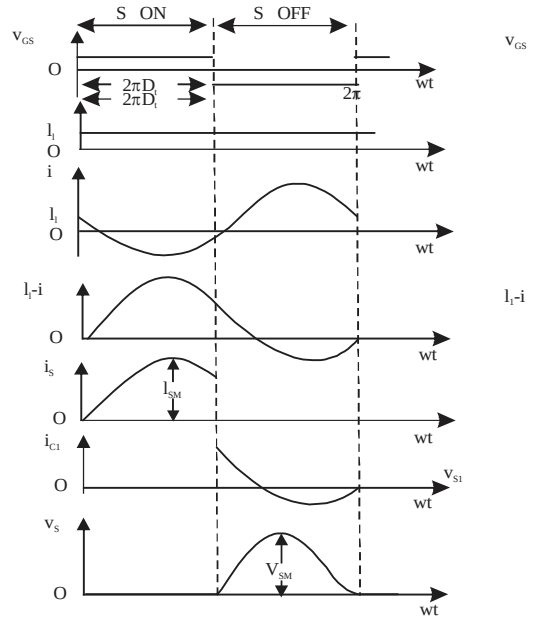

Fig. 3: Optimum operation waveforms in class E ZVS inverter in Kazimierczuk and Dariusz[18]

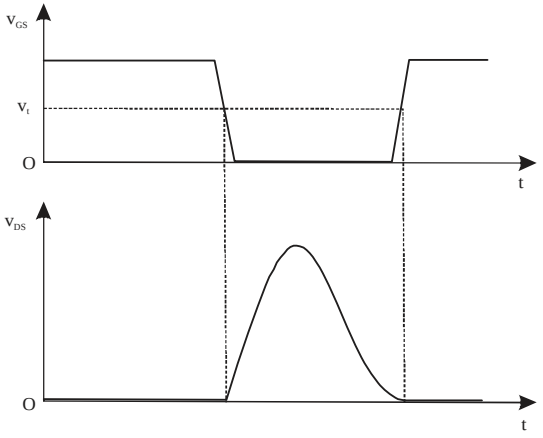

Fig. 4: Relationship of v_{GS} and v_{DS} waveforms for class E ZVS inverter

switch turns on, the switch current is increased gradually from zero after the switch is closed. For optimum operation, the switch voltage and the switch current are at positive level thus eliminating the requirement of additional diode to the switch.

The waveforms of gate-to-source voltage v_{GS} and drain-to-source voltage v_{DS} for operation of ZVS in the class E inverter is depicted in the Fig. 4. The operation must satisfy this condition in order to achieve high efficiency inverter.

The equation involved in component's value in the optimum operation at duty cycle, D = 0.5 is obtained and altered from Kazimierczuk and Dariusz[18] as below.

The AC load of the inverter can obtained:

$$R_i = \frac{8V_1^2}{(\pi^2+4)P_{Ri}} \quad (1)$$

The value of shunt capacitor:

$$C_1 = \frac{I_0}{\omega\pi V_1^2} = \frac{1}{\omega R_i\left(\frac{\pi^2}{4}+1\right)\frac{\pi}{2}} \quad (2)$$

The value of series capacitor (from L, C, R_i resonant circuit):

$$C = \frac{1}{\omega R_i\left(Q-\frac{\pi(\pi^2-4}{16}\right)} \quad (3)$$

The value of choke inductor:

$$L_f = 2\left(\frac{\pi^2}{4}+1\right)\frac{R}{f} \quad (4)$$

The value of series inductor:

$$L = \frac{QR_i}{\omega} \quad (5)$$

In order to calculate the voltage at the AC load:

$$V_{Ri(maximum)} = V_1\frac{4}{\sqrt{\pi^2+4}} \quad (6)$$

The switch voltage can be calculated as:

$$V_{s(maximum)} = 3.562\ V_1 \quad (7)$$

The current that flows in the choke inductor:

$$I_f = \frac{8}{\pi^2+4}\left(\frac{V_1}{R_i}\right) \quad (8)$$

The current that flows in an AC load can be calculated as:

$$I_{Ri} = \left(\frac{\sqrt{\pi^2+4}}{2}\right)I_{Lf} \quad (9)$$

The voltage at the series-resonant capacitor:

$$V_{C(maximum)} = \frac{I_{Ri(maximum}}{2\pi fC} \quad (10)$$

The voltage at the series-resonant inductor:

$$V_{L(maximum)} = 2\pi\ fL\ (I_{Ri\ (maximum)}) \quad (11)$$

The switch current can be obtained using:

$$I_{S(maximum)} \left(\frac{\sqrt{\pi^2+4}}{2} + 1 \right) I_{Lf} \quad (12)$$

The rms value of switch current as per below:

$$I_{S(rms)} = \left(\frac{\sqrt{\pi^2+28}}{4} \right) I_{Lf} \quad (13)$$

As, the effect on the switch conduction loss 2:

$$P_{rDs} = I^2_{S(rms)\times rDs} \quad (14)$$

Optimum operation can only be achieved at optimum load resistance, $R_i = R_{opt}$.

Stage 2: Optimum operation of class E ZVS with attached piezoelectric transducer

Theoretical calculation: In the earlier explanation, an AET system requires the piezoelectric transducer at the transmitter unit to convert an electrical energy to pressure wave/sound wave/vibration energy before the energy can be transmitted via any medium wirelessly. In this part, an equivalent circuit of piezoelectric transducer is attached to the end of the inverter. Fig. 5 shows the typical equivalent electrical circuit of piezoelectric transducer that used in this stage. Details explanation regarding the modeling are stated by Abdullah *et al.*[21] and Fabijanski and Lagoda[22].

The static capacitance of the piezoelectric transducers is adopted from Abdullah *et al.*[21] can be calculated as:

$$C_S = \frac{K^T_{33}\varepsilon_0\pi r^2}{h} \quad (15)$$

The value of K^T_{33} is assumed to be 635 as gained from piezoelectric calculator developed by APC international, Ltd. The value of C_T, L_T and R_{PZT} can be obtained using relevant information from the manufacturer datasheet for piezoelectric transducer. In this study, the piezoelectric transducer with a part number of MCUSD11A400B11RS from multicomp is applied.

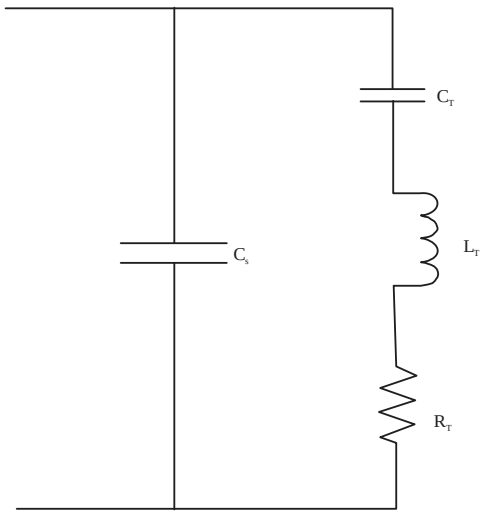

Fig. 5: Typical series-resonance equivalent circuit for piezoelectric transducer

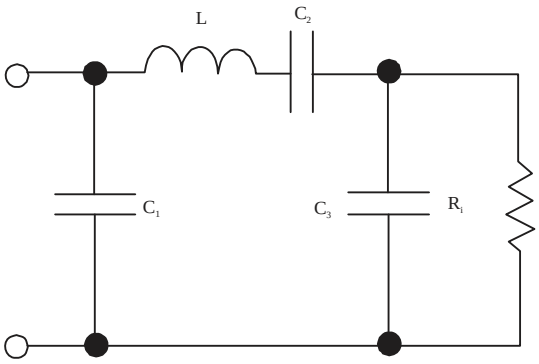

Fig. 6: Equivalent circuit of the matching circuit π1a

Stage 3: Optimum operation of class E ZVS with attached piezoelectric transducer with a matching impedance

Theoretical aspect: The power delivered to a load is maximized when the load impedance if equal to source load as stated in Svilainis and Dumbrava[16] and Kazimierczuk and Dariusz[18]. On the previous stage, the value of AC load is changed, thus the load impedance is not equal to the source load. Therefore, it is required for matching circuits that provide impedance transformation. Impedance transformation can be accomplished whether by tapping the resonant capacitance or resonant inductance as explained by Kazimierczuk and Dariusz[18]. This study implemented resonant circuit π1a for the design that shown in Fig. 6.

In order to obtain the components value of matching circuit, we will use the value of PZT load resistance, 173.06 Ω as the value of R_i.

The series equivalent resistance, R_s can be obtained using:

$$R_S = \frac{8}{\pi^2+4}\frac{V_1^2}{P_{Ri}} \approx 0.5768\frac{V_1^2}{P_{Ri}} \quad (16)$$

The reactance factor for the R_i-C_3 and R_s-C_s equivalent two-terminal networks is:

$$q = \frac{R_i}{X_{C3}} = \frac{X_{C_S}}{R_S} \quad (17)$$

The relationship between R_s and R_i will develop the reactances of X_{Cs} and X_{C3}:

$$R_S = \frac{R_i}{1+q^2} = \frac{R_i}{1+\left(\frac{R_i}{X_{C3}}\right)^2} \quad (18)$$

$$X_{CS} = \frac{X_{C3}}{1+\frac{1}{q^2}} = \frac{X_{C3}}{1+\left(\frac{X_{C3}}{R_i}\right)^2} \quad (19)$$

Rearrangement of Eq. 18 results in:

$$q = \sqrt{\frac{R_i}{R_S}-1} \quad (20)$$

Thus, by substituting the Eq. 20 into Eq. 17, resulting in:

$$X_{CS} = R_S\sqrt{\frac{R_i}{R_S}-1} \quad (21)$$

The DC input resistance of the class E inverter can be obtained through:

$$R_{DC} = \frac{V_1}{I_1} = \frac{(1-D)[\pi(1-D)\cos\pi D + \sin\pi D]}{\omega C_1 \tan(\pi d+\phi)\sin\pi D} \quad (22)$$

Using Eq. 21 and 22, one can obtain:

$$X_{C2} = \frac{1}{\omega C_2} = R_S\left[Q_L - \frac{\pi(\pi^2-4)}{16} - q\right] \quad (23)$$

Thus, yielding:

$$X_{C3} = \frac{1}{\omega C_3} = \frac{R_i}{q} = \frac{R_i}{\sqrt{\frac{R_i}{R_s}-1}} \quad (24)$$

Based on Eq. 23 and 24, the value of C_2 and C_3 of matching circuit can be calculated.

RESULTS AND DISCUSSION

The analysis of class E ZVS inverter of Fig. 2 is carried out under the following assumptions:

- The transistor and diode form an ideal switch whose on-resistance is zero, off-resistance is infinity and switching time is zero
- The choke inductance is high enough so that its ac component is much lower than the DC component of the input current
- The loaded frequency Q_L of the L-C-R_i series-resonant circuit is high enough so that the current i through the resonant circuit is sinusoidal

Stage 1: Optimum operation of class E ZVS

Theoretical result: In the first stage, the theoretical value of each component is found using the Eq. 1-13 based on the design specifications for Fig. 2 which is as follows: DC input voltage = 3.6 V, operating frequency = 416 kHz, power at the AC load, P_{Ri} = 0.08 W, rDs = 0.12 Ω, Q = 10. The theoretical value of the components in the inverter circuit is shown in Table 2.

Table 2: Theoretical value of inverter components for optimum operation

Component of the inverter	Values
R_i	93.44 Ω
C_1	0.752 nF
C	0.463 nF
L_f	1557.692 µh
L	357.493 µh
$V_{Ri(maximum)}$	3.867 V
$V_{S(maximum)}$	12.823 V
I_f	0.022 A
$I_{Ri(maximum)}$	0.041 A
$V_{C(maximum)}$	34.210 V
$V_{L(maximum)}$	38.666 V
$I_{S(maximum)}$	0.064 A
P_{rDs}	0.001 W

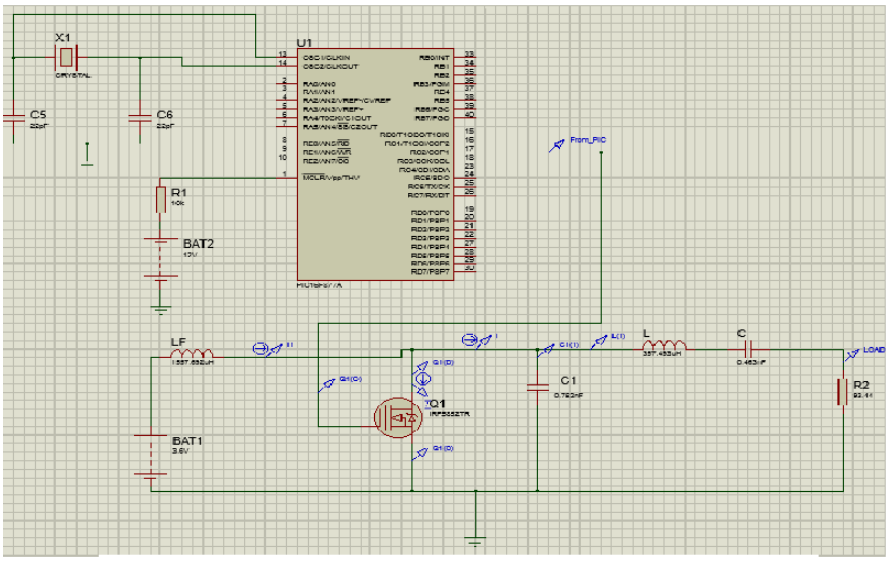

Fig. 7: Simulation model of optimum operation class E ZVS inverter

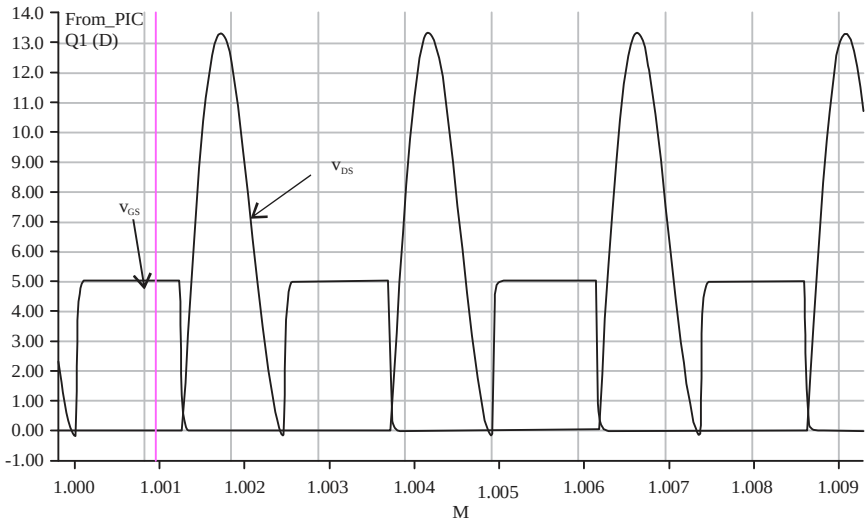

Fig. 8: Generation of PWM and ZVS condition fulfillment simulation results for optimum operation

Simulation results: In order to verify the working principle of class E ZVS inverter, the simulation model is developed using the Proteus software. A simulation model for this optimum operation of class E ZVS along with the PWM generator for MOSFET IRF5852TR is shown in Fig. 7.

The simulation result of PWM generation as illustrated by square waveform is shown in Fig. 8. This is a stable waveform with 5 Vp-p and 2.4 μS duration for 1 cycle. This signal will turn on and off the MOSFET thus drive the piezoelectric transducer to perform the electrical signal to pressure wave conversion at the operating frequency of 416 kHz. Figure 8 also shown the accomplishment of ZVS condition whereby the theoretically, there is no overlapping of switch current and voltage waveform during the switching time intervals, thus the switching losses are virtually zero, producing high efficiency. However, in simulation due some parasitic resistance value setting in the components, small overlapping occurred and this small disturbance is omitted in this study. This simulation fulfilled the ZVS requirement as illustrated in Fig. 4, thus it can be concluded that the high efficiency of inverter performance is achieved in this particular simulation.

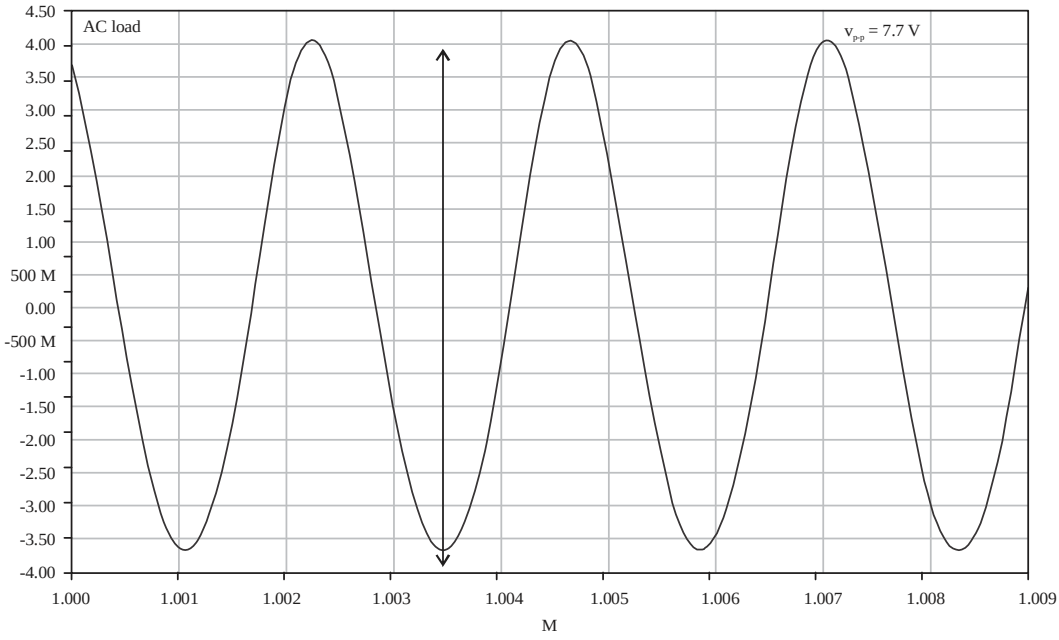

Fig. 9: Output voltage waveform at AC load of the inverter

Table 3: Electrical equivalent circuit component's value

Components	Values
C_S	2.136 nF
C_T	569.73 pF
L_T	257 µh
R_{PZT}	671.52 Ω
Total impedance value of PZT	173.06 Ω

As our main attention in this study is to produce ac output voltage, the Fig. 9 shows the voltage waveform that measure at the AC load resistor. It can be seen that the circuit able to convert the dc source to an ac source that will be transferred wirelessly. From the calculation, the value of $V_{Ri(maximum)}$ is 3.867 V meanwhile in simulation, the value is 3.85 V. In order to calculate the power, the basic equation of $P_{output} = \frac{V_{orms}^2}{R_i}$ is implemented. The calculation gave us 80 mW whereas, in the simulation, the power output voltage obtained is 79.3 mW.

Stage 2: Optimum operation of class E ZVS with attached piezoelectric transducer

Theoretical calculation results: Table 3 displayed the theoretical value of components for equivalent electrical circuit for piezoelectric transducer. The value of static capacitance, C_S is calculated from Eq. 15, whereas, for C_T, L_T and R_{PZT} are obtained from manufacturer datasheet. This mentioned value will be used in the simulation model that bring together the class E ZVS inverter and the piezoelectric transducer that supposed be as in the real applications.

Simulation results: After the extension of the optimum operation class E ZVS inverter with the equivalent electrical circuit of piezoelectric transducer, the changing in output voltage is expected due to the change of the total impedance. In the optimum operation section, only pure resistive impedance with the value of 93.442 Ω is applied. However, in this stage, the equivalent electrical circuit of piezoelectric transducer consists of inductor, capacitor, static capacitor and resistor that contributed to the overall variation in the impedance value. Here, the previous ac load of class E ZVS inverter, 93.442 Ω is replaced with a complete of PZT transducer equivalent circuit while the other components of the inverter are maintained as shown in Fig. 10. The total impedance value of PZT transducer equivalent circuit that illustrated in Fig. 5 has been calculated and being used for further analysis.

Figure 11 illustrates the ZVS condition of the simulation result after the addition of PZT equivalent circuit. The non-overlapping of the switch time intervals still maintained as before. However, small distortion occurred at the switch voltage waveform due to mismatch problem. Here, the changed of resulted waveform due to the addition of the PZT equivalent electrical circuit is expected. As compared to Fig. 8 and 12 shows the output voltage that measured at the total impedance of PZT transducer, not at the AC load of inverter as in previous measurements. From the obtained of v_{peak} = 3.85 V, in this stage, the simulation model only managed to get 42.83 mW that based on

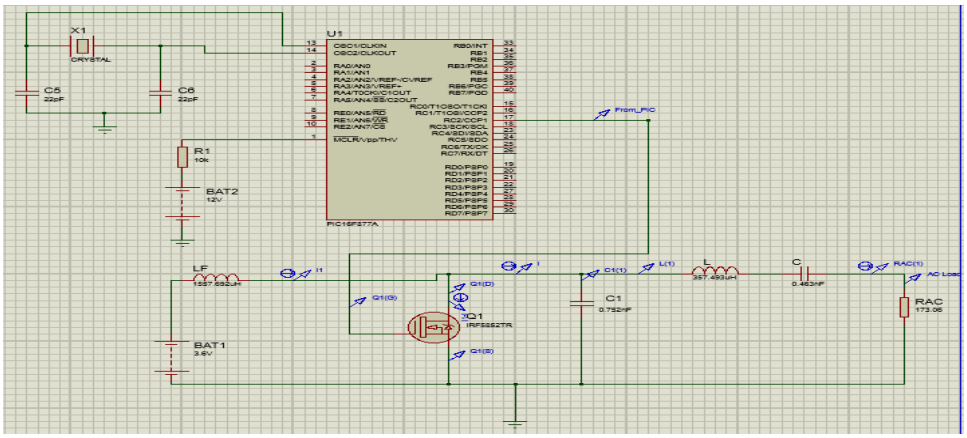

Fig. 10: Class E ZVS inverter attached to a simplified PZT equivalent circuit

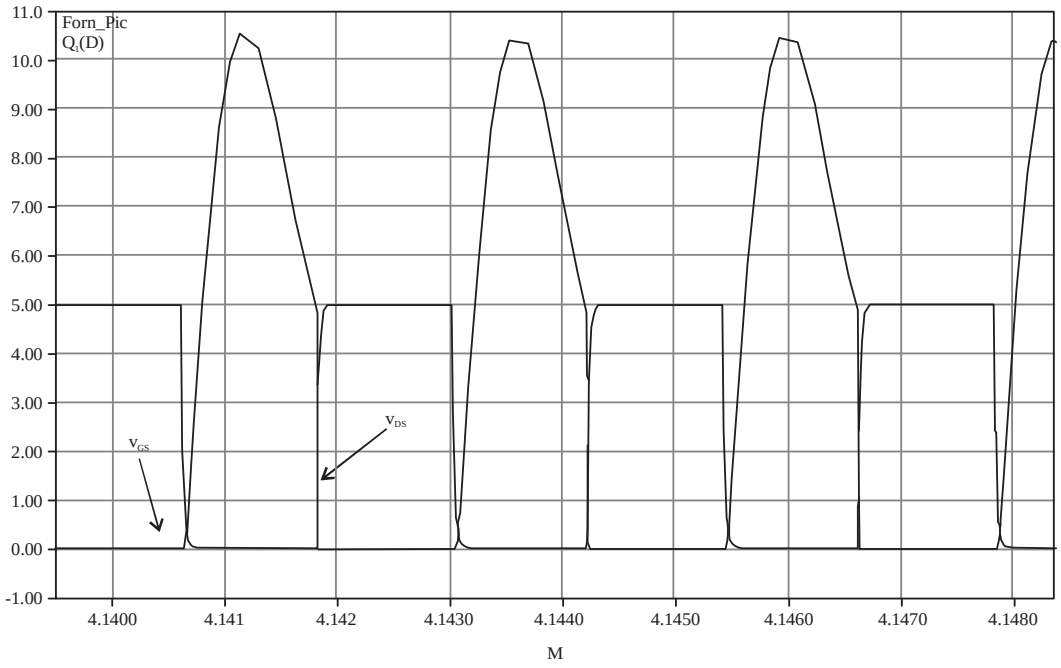

Fig. 11: ZVS condition of the inverter with PZT attached

$P_{output} = \frac{V_{orms}^2}{R_i}$ equation. With an efficiency of 53.53%, it is moreover remote from the main objective. This major reduction in the power output is mainly due to the mismatch of impedance for optimum operation. From the first stage simulation result, we obtained the load for optimum operation is 93.44 Ω, meanwhile in this stage; the total impedance of PZT transducer is 173.06 Ω. It is stated in Kazimierczuk and Dariusz[18] that if the value of load resistance is higher than the optimum resistance, the inverter will operates in the non-optimum region. This will be improved using the impedance matching technique that described earlier.

Stage 3: Optimum operation of class E ZVS with attached piezoelectric transducer with a matching impedance circuit

Theoretical calculation results: Some of important equations are outlined as Eq. 16-24 in order to obtain the matching impedance circuit component's value. Table 4 displayed the value of relevant components of the resonant circuit π1a. The other component values in Fig. 10 are maintained as calculated earlier. Meanwhile, the total impedance value of 173.6 Ω will be used as load resistance of the circuit. The circuit simulation model of stage 2 is modified to be similar as an equivalent circuit for π1a matching circuit as shown in Fig. 6.

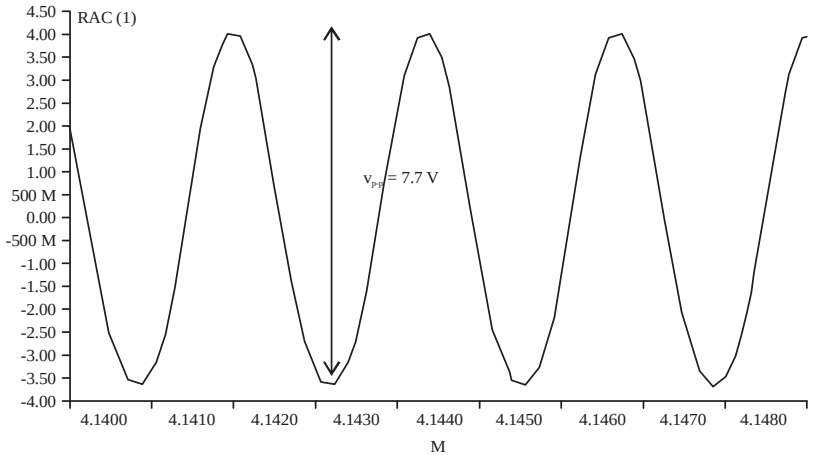

Fig. 12: Output voltage waveform at the PZT transducer

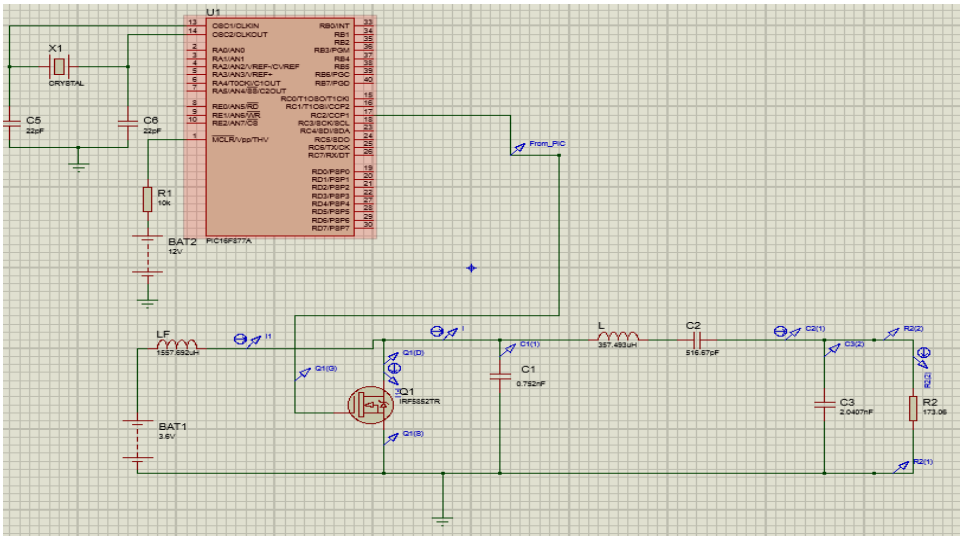

Fig. 13: Complete simulation model of transmitter unit

Table 4: Impedance circuit π1a component's value

Component	Values
C_2	516.67 pF
C_3	2.0407 nF
R_i	173.06 Ω

Simulation results: From the component values in Table 4, the model of complete transmitter unit that consists of an inverter, matching impedance and piezoelectric equivalent electrical circuit is simulated accordingly. Figure 13 displays the complete model of the simulation for the transmitter unit. The model observed to be less complicated due to the simplified version of the piezoelectric transducer circuit as compared to Fig. 5. Thus, the analysis and calculation will be shortened and easier for the beginners in this field.

In order to achieve high efficiency inverter, the natures of class E ZVS must be always satisfied. The non-overlapping transition between the switch current and voltage waveforms must be fulfilled all the time. This simulation result managed to satisfy the ZVS requirement as elaborated in Fig. 14. In Fig. 14, the simulation result also shown that the ZVS waveform is successfully recovered as resulted in the Fig. 8 whereby the inverter operated in the optimum condition. Therefore, it can be concluded that the high efficiency inverter performance is feasible and achievable.

As our main concerns, the output power that produced at the pzt transducer as a load of the transmitter unit. This power will transfer wirelessly to the receiving transducer at the receiver unit. Figure 15 presents the output voltage that is

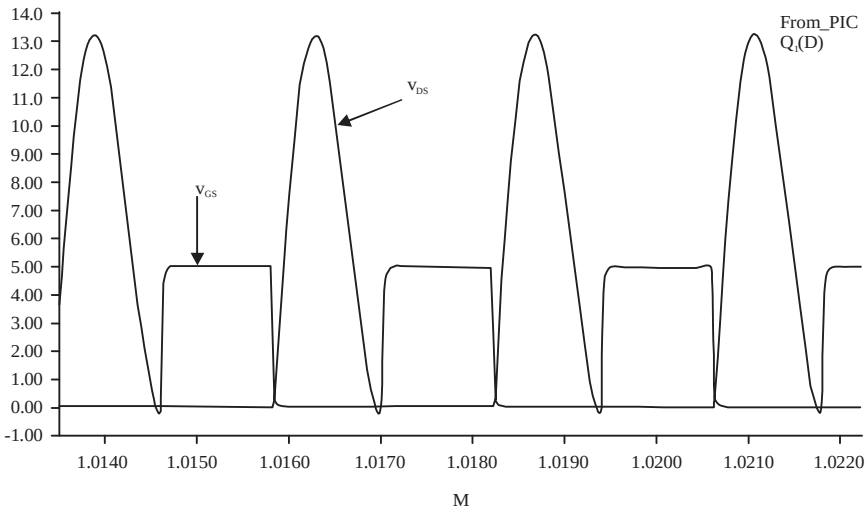

Fig. 14: ZVS waveform of complete transmitter unit simulation model

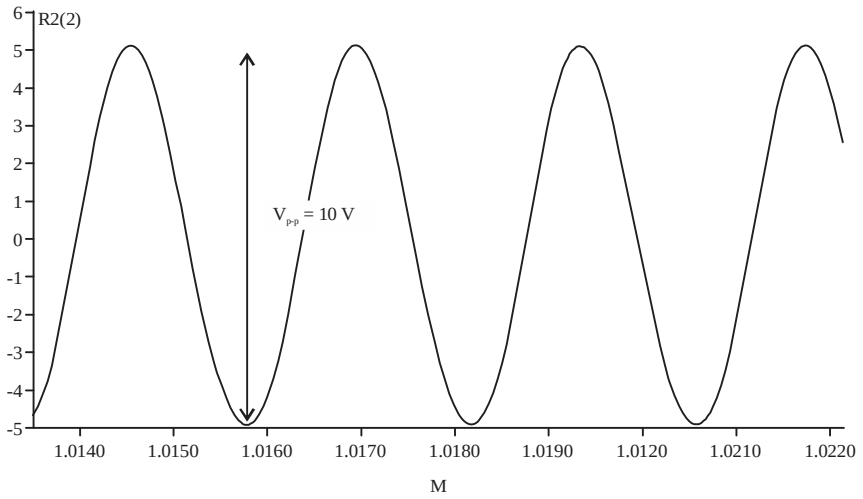

Fig. 15: Output voltage waveform of piezoelectric transducer load

measured at the PZT transducer. The inverter with complete matching impedance circuit gives 10 V as peak-to-peak voltage. With the PZT load impedance of 173.06 Ω, the output power obtained is 72.22 mW, which can be considered as a better performance. This value is closer to 80.0 mW that being aimed as the inverter output in this research. With the help of an impedance matching circuit, the transmitter unit of this AET system succeeded to gain 90.3% efficiency. This finding is aligned with the proposed efficiency as suggested by Ozeri and Shmilovitz[4].

CONCLUSION

The performance of transmitter unit that consists of class E ZVS inverter and piezoelectric transducer at the operating frequency of 416 kHz is studied, simulated using Proteus and compared. The simulation of performance for optimum operation of class E ZVS inverter, followed by adding the piezoelectric transducer and lastly is ending with the impedance matching circuit provides the guideline for those that required such knowledge. The step-by-step and simple designs are illustrated and shown that the feasibility and capability of inverter to achieve a high efficiency power conversion that can be improved by add in the matching impedance to the existing circuit. The complete AET transmitter unit managed to obtain 72.22 mW as the inverter output power. As the main target of the study, higher power conversion efficiency at the transmitter unit of 90.3% is achieved and it is being calculated as the ratio of output power to input power. The high efficiency performance is

realized through the satisfaction of class E ZVS inverter operation requirement throughout the simulation works.

NOMENCLATURE

ε_0 = Vacuum permittivity (8.85×10^{-12} F m^{-1})
r = Radial of piezoelectric surface (m)
K_{33}^{T} = Dielectric relative permittivity
h = Thickness of the piezoelectric (m)

ACKNOWLEDGMENTS

The authors would like to express an appreciation to Ministry Of Education Malaysia and Universiti Teknikal Malaysia Melaka (UTeM) for funding this research under RAGS/1/2014/TK0'3/FKEKK/B00062 grant.

REFERENCES

1. Hu, A.P., Z.J. Chen, S. Hussmann, G.A. Govic and J.T. Boys, 2002. A dynamically on-off controlled resonant converter designed for coalmining battery charging applications. Proceedings of the International Conference on Power System Technology, Volume 2, October 13-17, 2002, Kunming, China, pp: 1039-1044.
2. Roes, M.G.L., J.L. Duarte, M.A.M. Hendrix and E.A. Lomonova, 2013. Acoustic energy transfer: A review. IEEE Trans. Indus. Electron., 60: 242-248.
3. Sanni, A. and A. Vilches, 2013. Powering low-power implants using PZT transducer discs operated in the radial mode. Smart Mater. Struct., Vol. 22. 10.1088/0964-1726/22/11/ 115005
4. Ozeri, S. and D. Shmilovitz, 2010. Ultrasonic transcutaneous energy transfer for powering implanted devices. Ultrasonics, 50: 556-566.
5. Denisov, A. and E. Yeatman, 2010. Ultrasonic vs. inductive power delivery for miniature biomedical implants. Proceedings of the International Conference on Body Sensor Networks, June 7-9, 2010, Singapore, pp: 84-89.
6. Zaid, T., S. Saat, Y. Yusop and N. Jamal, 2014. Contactless energy transfer using acoustic approach-A review. Proceedings of the International Conference on Computer, Communications and Control Technology, September 2-4, 2014, Langkawi, Malaysia, pp: 376-381.
7. Karalis, A., J.D. Joannopoulos and M. Soljacic, 2008. Efficient wireless non-radiative mid-range energy transfer. Ann. Phys., 323: 34-48.
8. Kurs, A., A. Karalis, R. Moffatt, J.D. Joannopoulos, P. Fisher and M. Soljacic, 2007. Wireless power transfer via strongly coupled magnetic resonances. Science, 317: 83-86.
9. Theodoridis, M.P., 2012. Effective capacitive power transfer. IEEE Trans. Power Electron., 27: 4906-4913.
10. Liu, C., A.P. Hu and M. Budhia, 2010. A generalized coupling model for capacitive power transfer systems. Proceedings of the IECON 2010-36th Annual Conference on IEEE Industrial Electronics Society, November 7-10, 2010, Glendale, AZ., pp: 274-279.
11. Kline, M., I. Izyumin, B. Boser and S. Sanders, 2011. Capacitive power transfer for contactless charging. Proceedings of the 26th Annual Applied Power Electronics Conference and Exposition, March 6-11, 2011, Fort Worth, TX., pp: 1398-1404.
12. Chen-Yang, X., L. Chao-Wei and Z. Juan, 2011. Analysis of power transfer characteristic of capacitive power transfer system and inductively coupled power transfer system. Proceedings of the 2011 International Conference on Mechatronic Science, August 19-22, 2011, Jilin, China, pp: 1281-1285.
13. Jiang, H., J. Zhang, D. Lan, K.K. Chao, S. Liou and H. Shahnasser, 2013. A low-frequency versatile wireless power transfer technology for biomedical implants. IEEE Trans. Biomed. Cir. Syst., 7: 526-535.
14. Miller, J.L., 2014. Wireless power for tiny medical implants. Phys. Today, 67: 12-14.
15. Semsudin, N.A.A., J. Sampe, M.S. Islam and A.R.M. Zain, 2015. Architecture of ultra-low-power micro energy harvester using hybrid input for biomedical devices. Asian J. Sci. Res., 8: 212-224.
16. Svilainis, L. and V. Dumbrava, 2007. Evaluation of the ultrasonic transducer electrical matching performance. Ultrasound, 62: 16-21.
17. Nayak, D.K. and S.R. Reddy, 2011. Performance of the push-pull LLC resonant and PWM ZVS full bridge topologies. J. Applied Sci., 11: 2744-2753.
18. Kazimierczuk, M.K. and C. Dariusz, 2012. Class E Zero Voltage Switching Resonant Inverter.. In: Resonant Power Converters, Kazimierczuk, M.K. and D. Czarkowski, John Wiley and Sons, New Jersey, ISBN-13: 9781118585863 pp: 334-363.
19. Li, Y.F. and S.M. Sue, 2011. Exactly analysis of ZVS behavior for class E inverter with resonant components varying. Proceedings of the 2011 6th IEEE Conference on Industrial Electronics and Applications, June 21-23, 2011, Beijing, China pp: 1245-1250.
20. Xiaoyuan, W. and Y. Zhe, 2012. Simulation of ZVS converter and analysis of its switching loss based on PSPICE. Int. J. Power Elect. Drive Syst., 2: 19-19.
21. Abdullah, A., A. Pak and A. Shahidi, 1986. Equivalent electrical simulation of high-power ultrasonic piezoelectric transducers by using finite element analysis. Ultrasonic. Co. Ir.
22. Fabijanski, P. and R. Lagoda, 2011. Modeling and Identification of Parameters the Piezoelectric Transducers in Ultrasonic Systems. In: Advances in Ceramics-Electric and Magnetic Ceramics, Bioceramics, Ceramics and Environment. Sikalidis, C. (Ed.)., InTech, Osaka, ISBN: 978-953-307-350-7.